Experimental Study on the Corrosion Rate of High-strength Steel Wires in Main Cables of Suspension Bridges Under Service Conditions

Xiaoyu CHEN *

School of Civil Architecture and Environment, Chengdu Textile College, Chengdu 611731, Sichuan, China

http://doi.org/10.5755/j02.ms.40923

Received 24 March 2025; accepted 6 May 2025

To predict the corrosion progression of high-strength steel wires in the main cables of suspension bridges, this study proposes a method for calculating the corrosion rate of steel wires under service conditions. First, the corrosion rate was experimentally determined using a three-electrode system under orthogonal test conditions, varying the concentration of NaCl, pH, and tensile stress. The results reveal that both pH and NaCl concentration significantly influence the corrosion rate, with a notable coupling effect, while tensile stress has a relatively minor impact. A fitted calculation model was established to describe the relationship between these factors and the steel wire corrosion rate. Second, to validate the model, the environmental conditions of the Humen Bridge in China were analyzed. The annual corrosion rate of steel wires in this environment was estimated to be approximately 0.017 mm/year. Lastly, the diameter loss of the most severely corroded outer steel wire in the Humen Bridge's main cable was measured to be around 0.2 mm, aligning well with the model's predictions. Through experimental investigation and real-world validation, this study establishes a calculation method for predicting steel wire corrosion in suspension bridge main cables based on the internal cable environment and tensile stress. This method offers a novel approach for assessing and monitoring main cable corrosion in suspension bridges.

Keywords: corrosion rate calculation, suspension bridge main cable, orthogonal experiment.

1. INTRODUCTION

The main cables of suspension bridges are composed of thousands of high-strength steel wires, which serve as the primary load-bearing components of the structure [1 – 4]. However, corrosion of these steel wires within the main cable poses a significant threat to traffic safety [2 – 5]. Corrosion inspections of main cables have been conducted in the United States, Europe, and Japan, revealing alarming findings. For example, zinc coatings on steel wires typically corrode within 6–10 years of service, and after 30 years, the steel wire substrate experiences severe corrosion [6]. Accordingly, the National Cooperative Highway Research Program (NCHRP) Report 5347 [8], recommends that for suspension bridges in service for more than 30 years, external protective layers should be removed, main cables should be opened, corroded steel wires extracted, and their corrosion status evaluated. While this is a common method for main cable inspection, it can lead to secondary damage and is incapable of assessing the condition of inner steel wires [8, 9].

The corrosion of steel wires is primarily driven by the surrounding environment and the tensile stress applied to the wires [10, 11]. Previous studies have extensively explored the factors influencing corrosion. For instance, the behavior of duplex stainless steel under the influence of chloride ions has been investigated, with findings showing that lower chloride concentrations tend to cause pitting at the rebar level, while higher solution temperatures (> 50 ℃) can exacerbate corrosion [12, 13]. Research on the corrosion fatigue of steel wires under live load stress indicates that the greater the degree of corrosion, the steeper the S-N curve, and abrupt changes may occur under high-stress amplitudes [14 – 16]. Additionally, the relationship between temperature, humidity, and the corrosion rate of steel wires has been established [17]. A comprehensive analysis of factors affecting steel wire corrosion identified temperature, relative humidity, tensile stress, pH value, and chloride concentration as the most significant contributors [17 – 19]. While these studies offer valuable insights and recommendations for reducing the corrosion rate of main cables, they lack a quantitative model correlating environmental factors with corrosion rate, limiting their application in practical corrosion calculations.

This study aims to address this gap by conducting orthogonal experiments to investigate the effects of chloride concentration, pH value, and tensile stress on the corrosion rate of steel wires. The corrosion rate under each orthogonal test condition was measured to determine potential coupling effects among these factors. A comprehensive quantitative relationship between environmental factors and the steel wire corrosion rate was then established.

The instantaneous corrosion rate of steel wires was measured using an electrochemical method. However, traditional electrolytic devices are unable to simulate tensile stress on steel wires during measurement, as previous studies typically assessed corrosion rates after releasing the tensile force—an approach inconsistent with the actual service conditions of bridges. To overcome this limitation, a self-balanced tension frame was designed. This innovation allows electrochemical corrosion rate measurements of steel wires under varying levels of tensile stress, enabling more

* Corresponding author: X. Chen
E-mail: *ChenXiaoyu@ctc-edu.cn*

accurate simulations of in-service conditions. Finally, the experimental results were validated by comparing them with corrosion data from the Humen Bridge, predicting the diameter loss caused by steel wire corrosion. This provides a valuable reference for the anti-corrosion maintenance of suspension bridge main cables.

2. EXPERIMENTAL PROCEDURE

To establish a calculation model correlating the corrosion rate of steel wires with NaCl concentration, pH value, and tensile stress, orthogonal experiments were designed. These experiments measured the instantaneous corrosion rate of steel wires under various test conditions.

2.1. Experimental samples

To align with the temperature, humidity, and corrosion rate calculation model established in literature [8], the experimental samples were selected from the same batch of steel wires. These non-galvanized, high-strength steel wires (1770 MPa) were manufactured by Shanghai Baogang Group for suspension bridge main cables. The wire diameter is 5.10 mm. The chemical composition of the steel wires is as follows: C 0.83 %, Mn 0.75 %, Si 0.007 %, P 0.008 %, Cr 0.14 %, Cu 0.03 %, and Fe (balance).

All samples were prepared by grinding with SiC paper up to 1000 grits, followed by cleaning with deionized water, ultrasonic cleaning in ethanol, and air-drying.

2.2. Design of experimental conditions

The test values for the three corrosion factors – NaCl concentration, pH value, and tensile stress – were selected to simulate the service environment of bridges.

NaCl concentration (g/L): values ranged from 0.1 %–0.7 % (coastal atmosphere) to 3.2 %–3.75 % (seawater salinity), adjusted using NaCl crystals to prepare the Cl^- solution. pH value: spanned from 4 (severe acid rain) to 8 (seawater), adjusted using HCl for acidic electrolytes and NaOH for alkaline electrolytes. Tensile stress: calculated with a safety factor of 2.0, the maximum applied stress was 800 MPa. Temperature: held constant at 25 ℃ using a thermostatic controller.

The detailed test conditions are shown in Table 1.

Table 1. Values of orthogonal experiment factors

Value grade	NaCl concentration, g/L	pH value	Tensile stress, MPa
MARK	*A*	*B*	*C*
1	0.3 %	4	400
2	0.9 %	5	500
3	1.8 %	6	600
4	2.6 %	7	700
5	3.5 %	8	800

2.3. Constant tension of steel wire

To simulate corrosion under tensile stress, a self-balanced reaction frame was designed to apply tensile stress to the steel wires. The experimental setup anchored both ends of the steel wire to a bottom plate via steel tubes. The tube width matched the spacing of the bottom plate holes to ensure uniform vertical tensile stress. The tension was applied using a hydraulic jack, with the tensile force monitored in real time by a BK48 pressure sensor connected to a Donghua DH3818N static stress-strain test analyzer. This system allowed precise control and stabilization of the tensile force. The design of the self-balancing reaction frame is shown in Fig. 1.

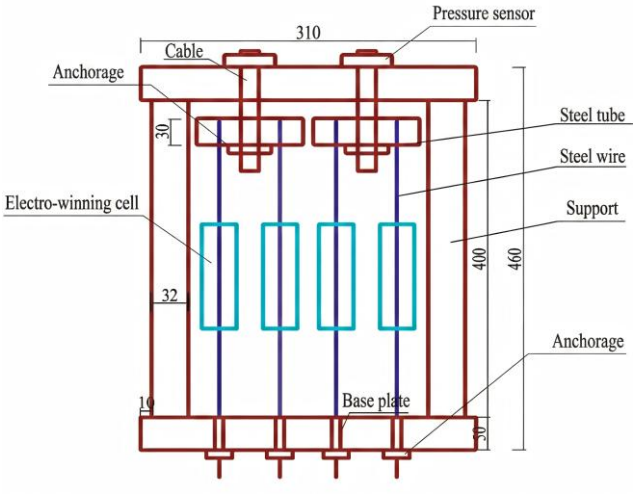

Fig. 1. Design drawing of the self-balancing reaction frame

To stabilize the applied tension, the jack was adjusted after an initial 10-minute stabilization period. Once the design stress was achieved and stabilized, the jack was removed, and the corrosion rate measurement began immediately.

2.4. Design of the electrolytic cell

A three-electrode system was employed in the experiment, consisting of: reference electrode: saturated calomel electrode; auxiliary electrode: platinum electrode; working electrode: steel wire under tensile stress.

The electrolytic cell was specifically designed to accommodate the steel wire under tension in a controlled temperature environment. The steel wire passed through the cell, where the solution temperature was maintained by a thermostatic controller, and the electrolyte was continuously circulated using a micro-pump. The design of the electrolytic cell is illustrated in Fig. 2.

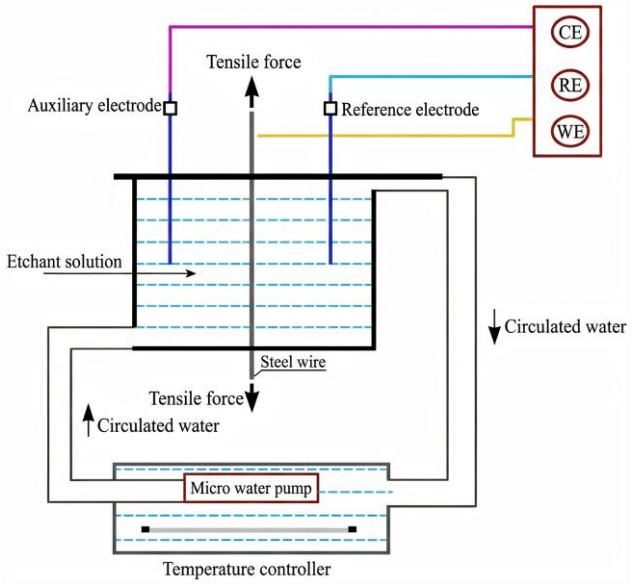

Fig. 2. Electrolytic cell design

The corrosion rate was measured using the CS320 corrosion rate test system, provided by Wuhan Koster Equipment Company. The Tafel curve extrapolation method was employed, using Tafel polarization potential scanning to determine the corrosion rate [12].

3. EXPERIMENTAL RESULTS

The experimental measurement focused on the instantaneous corrosion rate of the steel wire samples. Initially, the corrosion rate is higher but decreases slightly after the formation of corrosion products, which hinder oxygen diffusion. However, this transient phase is negligible compared to the steel wire's overall lifespan. Thus, the instantaneous corrosion rate of the stabilized wire is considered representative of its average lifetime corrosion rate [12].

3.1. Corrosion rate measurement

The corrosion rate was determined using the Tafel curve extrapolation method [12]. The parameters used in the experiment include a working electrode contact area of 11.50 cm^2, a sample steel wire density of 7.8 g/cm^3, and a chemical equivalent weight of 27.9 g (calculated as the molar mass divided by the number of electrons involved in the electrochemical reaction).

The scanning potential ranged from –0.3 V to 0.3 V, with a scanning rate of 10 $mV \cdot s^{-1}$. The reference electrode and auxiliary electrode were immersed in the electrolyte, and the system was allowed to stabilize for 1 – 2 minutes before polarization commenced. The Tafel curve for the sample steel wire under working condition 1-1-1 is shown in Fig. 3.

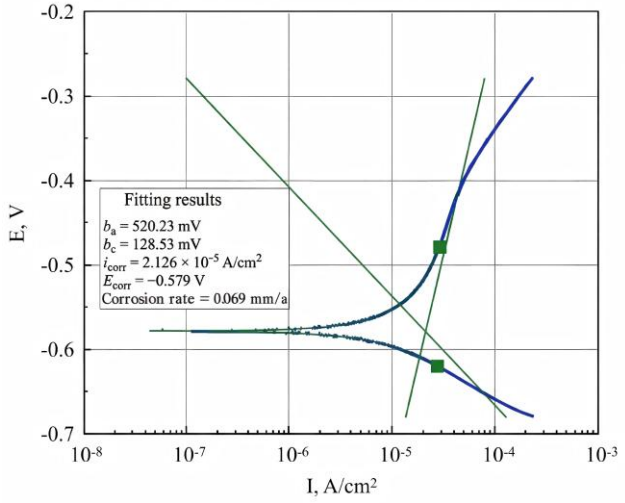

Fig. 3. Measurement data of the steel wire sample under working condition 1-1-1

Working condition 1-1-1 represents the following combination of factors: NaCl concentration at level 1 (0.3 %), pH at level 1 (4), and steel wire tension at level 1 (400 MPa).

From the E-lgi diagram obtained, the Tafel four-parameter fitting was employed to extract key parameters: b_a (anode curve slope), b_c (cathode curve slope), E_0 (self corrosion potential), i_0 (self corrosion current density). The Tafel slopes (β_a and β_c) were determined using the electrochemical workstation's fitting capabilities. The corrosion current density (i_{corr}) was calculated using Eq. 1 [11].

$$i = i_{corr}\left\{\exp\frac{E-E_0}{\beta_a} - \frac{\exp\frac{-(E-E_0)}{\beta_c}}{1-\frac{i_0}{i_L}[1-\exp\frac{-(E-E_0)}{\beta_c}]}\right\}, \quad (1)$$

where i is the external polarization current density; i_{corr} is the self-corrosion current density; i_L is the limiting current diffusion density; $E - E_0$ is the polarization potential; β_a and β_c are the Tafel slopes for the anodic and cathodic reactions.

Tafel slope is expressed by logarithm (lg), and anode and cathode slopes are expressed by $b_a = 2.303 \times \beta_a$, $b_c = 2.303 \times \beta_c$, respectively.

After determining the self-corrosion current density i_{corr} , the corrosion rate V_{corr} was calculated using Eq. 2.

$$V_{corr} = \frac{\Delta m}{S \cdot t} = \frac{A}{n \cdot F} \cdot i_{corr}, \quad (2)$$

where Δm is the mass of metal dissolved at the anode, g; i_{corr} is corrosion current intensity, A; A is the atomic weight of the metal; t is the power on time, s; n is the valence number (the number of electrons in the metal anode reaction equation); F is the faraday constant (1 F = 96500 C/mol); S is the surface area of the metal anode.

Using the above method, the calculated corrosion rate for the conditions shown in Fig. 3 was 0.0764 mm/year.

3.2. Judgment of coupling effect

Before conducting the orthogonal experiment, it was necessary to preliminarily assess whether a coupling relationship exists between NaCl concentration, pH value, and tensile stress in influencing the corrosion rate. The individual effects of the three factors are denoted as *A*, *B*, and *C*, respectively, as shown in Table 1. Pairwise coupling effects are represented as *AB*, *AC*, and *BC*, while the comprehensive coupling effect of all three factors is denoted as *ABC*.

The experimental approach involved combining the maximum and minimum limit values of the three factors: NaCl concentration, pH value, and tensile stress. This resulted in eight experimental conditions with limit values, each represented as *a*, *b*, *c*, *d*, *ab*, *ac*, *bc*, and *abc*, as illustrated in Fig. 4.

To quantify the influence of each factor, the mean change in the experimental index caused by varying each factor was calculated, representing the effect of the factor [11]. The formula for calculating the influence effect of factor A is as follows:

$$A = \frac{1}{4n}(a + ab + ac + abc - d - b - c - bc). \quad (3)$$

Similar formulas were used to calculate the effects of factors *B* and *C*. The formula for calculating the interaction effect of factors *AB* is as follows:

$$AB = \frac{1}{4n}(ab + abc + d + c - b - a - ac - bc). \quad (4)$$

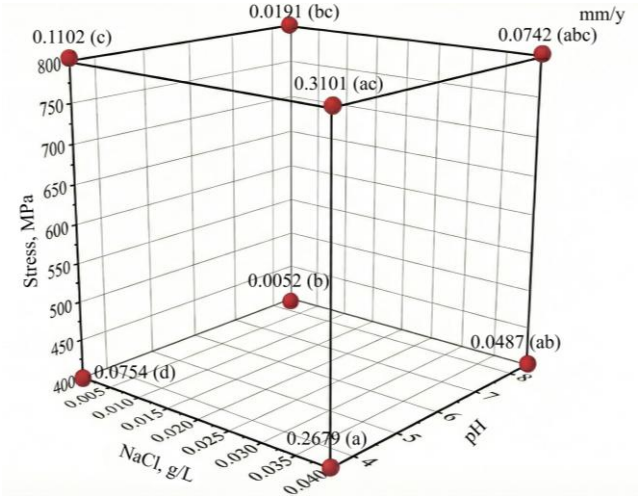

Fig. 4. Analysis of coupling effect

Similarly, the interaction effects of *BC* and *AC* were calculated using analogous formulas. Furthermore, the formula for calculating the combined effect of factors *ABC* is as follows:

$$ABC = \frac{1}{4n}(abc + a + b + c - d - ab - ac - bc). \quad (5)$$

From the calculations, the influence effects were determined as follows: Factor *A* (NaCl concentration): 0.5026; Factor *B* (pH value): –0.6280; Factor *C* (tensile stress): 0.1079; Pairwise interaction effects: *AB*: –0.2821, *AC*: 0.0273, *BC*: –0.0460; Comprehensive interaction effect (*ABC*): 0.0126.

Based on these results, the relative importance of the factors and their coupling effects was preliminarily ranked as follows: $B > A > AB > C > BC > AC > ABC$. That is to say, the effect of *B* (pH value) and *A* (NaCl concentration) on the corrosion rate of is greater than *C* (tensile stress), and the couple effect of *AB* (NaCl concentration and pH value) should be considered as a new factor to be investigated for orthogonal design. The influence of factor *C* (tensile stress) is greater than that of *ABC*, *AC* and *BC*, so the coupling effect of *BC*, *AC*, and *ABC* can be ignored.

3.3. Results of orthogonal experiment

The orthogonal experiment method [11] was used to combine three independent factors and one coupling factor, resulting in a total of 25 test conditions. For each condition, the average of three sample measurements was calculated. The experimental results are shown in Table 2.

For better observation, the experimental data were categorized into five groups based on the NaCl concentration, as shown in Fig. 5.

From Fig. 5, three key features can be observed:

1. The corrosion rate fluctuates with the variation of the three factors. The minimum corrosion rate is 0.0087 mm/y, and the maximum is 0.2072 mm/y, showing an increase of about 24 times.
2. The corrosion rate increases significantly as the NaCl concentration rises.
3. Under the same NaCl concentration, the lower the pH value, the greater the corrosion rate.

Table 2. Orthogonal experimental results

Num	NaCl concentration	pH value	NaCl+pH	Tensile stress	Corrosion rate experimental value, mm/year			Mean value, mm/year
1	1	1	1	1	0.0674	0.0746	0.0844	0.0754
2	1	2	2	2	0.0379	0.0456	0.0448	0.0428
3	1	3	3	3	0.0152	0.0163	0.0162	0.0159
4	1	4	4	4	0.0078	0.0094	0.0090	0.0087
5	1	5	5	5	0.0196	0.0190	0.0187	0.0191
6	2	1	2	3	0.1109	0.1009	0.1149	0.1089
7	2	2	3	4	0.0481	0.0562	0.0602	0.0548
8	2	3	4	5	0.0458	0.0491	0.0509	0.0486
9	2	4	5	1	0.0191	0.0240	0.0173	0.0201
10	2	5	1	2	0.0128	0.0158	0.0127	0.0137
11	3	1	3	5	0.1421	0.1493	0.1520	0.1472
12	3	2	4	1	0.0598	0.0786	0.0727	0.0703
13	3	3	5	2	0.0471	0.0586	0.0447	0.0501
14	3	4	1	3	0.0331	0.0507	0.0229	0.035
15	3	5	2	4	0.0302	0.0387	0.0251	0.0313
16	4	1	4	2	0.2159	0.1878	0.2179	0.2072
17	4	2	5	3	0.1164	0.1285	0.1578	0.1342
18	4	3	1	4	0.0651	0.0639	0.0649	0.0646
19	4	4	2	5	0.0427	0.0484	0.0453	0.0455
20	4	5	3	1	0.0336	0.0251	0.0205	0.0264
21	5	1	5	4	0.2321	0.3075	0.2849	0.2748
22	5	2	1	5	0.1582	0.2089	0.1876	0.1849
23	5	3	2	1	0.0817	0.1008	0.0534	0.0786
24	5	4	3	2	0.0326	0.0567	0.0917	0.0603
25	5	5	4	3	0.0216	0.0502	0.0742	0.0487

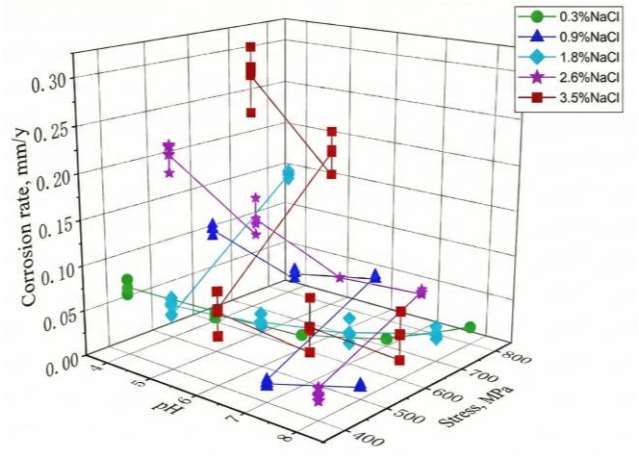

Fig. 5. Orthogonal experimental results

4. EXPERIMENTAL

By analyzing the data in Table 2, it is clear whether there is a coupling effect among the three factors, the primary and secondary relationships of their influence on corrosion, and their quantitative correlation with the corrosion rate.

4.1. Variance analysis

Variance analysis decomposes the total sum of squared variations into the squared variations caused by the experimental factors and errors. After eliminating the influence of errors, an *F*-test is used to determine the significance of each factor. The results of the variance and significance analysis are shown in Table 3 and Table 4, respectively.

Table 3. Variance analysis results

Factor	*A*	*B*	*AB*	*C*
*k*1	0.1519	0.8135	0.3736	0.2708
*k*2	0.2461	0.4870	0.3071	0.3741
*k*3	0.3339	0.2578	0.3046	0.3427
*k*4	0.4779	0.1696	0.3835	0.4342
*k*5	0.6473	0.1292	0.4883	0.4353
Q	0.1685	0.2022	0.1424	0.1418
S	0.0305	0.0642	0.0044	0.0038

$$K = \sum_{i=1}^{25} x_i = 1.8751 \quad P = \frac{1}{25} K^2 = 0.1380$$

$$W = \sum_{i=1}^{25} x_i^2 = 0.2468 \quad S = Q - P$$

Note: represent the sum of the test values of each factor under each value condition, while refers to the experimental data from Table 2 is the mean square sum of , and denotes the difference of the sum of squares. The calculation principles and methods are referenced in [11].

In Table 4, factors *A*, *B*, *AB*, and *C* are the four factors being investigated, and *e* represents the error. The degrees of freedom (DOF) for each factor are the number of value levels minus 1, the total DOF is the number of experimental conditions minus 1, and the error DOF is the sum of the total DOF minus the DOF for each factor. The calculation methods for variance adjustment, mean square, and *F* values are detailed in the literature [11].

By comparing the *F* values calculated in the table with the critical value (F_a), it can be determined that:

1. Factor *A* (NaCl concentration) is greater than the critical value at a 95 % confidence level, indicating that its effect on the corrosion rate is highly significant.
2. Factor *B* (pH value) exceeds the critical value at a 99 % confidence level, showing a significant effect on the corrosion rate.
3. However, the values of factor *AB* (coupling of NaCl concentration and pH value) and factor *C* (tensile stress) are less than the critical value at an 80 % confidence level, indicating that the influence of factor *AB* and factor *C* on the corrosion rate is not significant.

4.2. Fitting of calculation relationship of corrosion rate

To establish a calculation model correlating the three factors influencing corrosion with the corrosion rate of steel wires, the spline interpolation method was applied to the experimental data. A quadratic regression fitting was then performed to derive the corrosion rate regression formula.

MATLAB was used to interpolate the experimental data under the following conditions: NaCl concentration ranged from 0.3 % to 3.5 % with a step size of 0.5 %, pH value ranged from 4 to 8 with a step size of 0.5, and tensile stress ranged from 400 MPa to 800 MPa with a step size of 50 MPa.

A ternary quadratic regression function was employed to fit the interpolated data with 95 % confidence. Given the wide range of NaCl concentrations, a segmented fitting approach was adopted to ensure better accuracy. Specifically, different fitting functions were applied for NaCl concentrations greater than 1 and less than 1. The resulting regression Equations are expressed as follows (Eq. 3).

Table 4. Statistical significance of variance analysis

Source of variance	Squares sum of variation	DOF	Mean square	*F* value	Critical value, F_a	Significance
A	S_A = 0.0305	4	0.0076	10.86	$F_{0.05(4.24)}$=5.77	very significant
B	S_B = 0.0642	4	0.0161	23.00	$F_{0.01(4.24)}$=13.9	very significant
AB	S_{AB} = 0.0044	4	0.0011	1.57	$F_{0.2(4.24)}$=2.4	non-significant
C	S_C = 0.0038	4	0.0009	1.28	$F_{0.2(4.24)}$=2.4	non-significant
e	S_e = 0.0059	8	0.0007			
Total	S_T = 0.1088	24				

$$\begin{cases} V = 0.340242 + 0.00002x_{NaCl} - 0.08137x_{pH} - 0.00011x_t \\ +0.05933x_{NaCl}^2 + 0.005841x_{pH}^2 + 1.07\times10^{-7}x_t^2 - 0.0063x_{Nacl}x_{pH}\ (NaCl < 1) \\ V = 0.302428 + 0.129031x_{NaCl} - 0.15078x_{pH} + 0.000427x_t \\ +0.000967x_{NaCl}^2 + 0.012534x_{pH}^2 - 3.3\times10^{-7}x_t^2 - 0.01621x_{Nacl}x_{pH}\ (NaCl \geq 1) \end{cases}, \quad (3)$$

where V is the corrosion rate of uncoated smooth high-strength steel wire, mm/y; x_{NaCl} is concentration of NaCl, %; x_{pH} is the pH value of the solution (4 – 8); x_t is the tensile stress applied to steel wires, MPa.

In the Eq 3, the coefficient of tensile stress is relatively small because the stress values range from 400 to 800 MPa, which are significantly larger compared to other factors. The quadratic terms x_{NaCl} and x_{pH} represent coupling effects and cannot be ignored.

The accuracy and reliability of the fitting results were evaluated using reliability indices, as summarized in Table 5.

Table 5. Reliability index of fitting results

Fitting model	MCC	MDC	SD	SSD
NaCl < 1	0.9483	0.9785	0.0048	0.023
NaCl ≥ 1	0.9832	0.9213	0.0032	0.016

The calculation methods for Multiple Correlation Coefficient (MCC), Multiple Determinat Coefficient (MDC), Standard Deviation (SD), and Sum of Squares of Deviation (SSD) are detailed in reference [11]. The MCC measures the degree of correlation between the independent variables (x_{NaCl}, x_{pH}, x_t)and the dependent variable (V), with values of 0.9483 and 0.9832 indicating a strong positive correlation. The MDC reflects the proportion of variation in the dependent variable explained by the independent variables, with values of 0.9785 and 0.9213 suggesting that 97.8 % and 92.1 % of the variations are accounted for, respectively. The SD indicates the degree of fitting accuracy, where values below 0.005 demonstrate a high precision in the regression fit. Similarly, the SSD quantifies the deviation between the regression model and measured data, with values of 0.023 and 0.016 confirming minimal deviation and underscoring the reliability of the model. Overall, the regression analysis reveals a strong and reliable relationship between the corrosion rate and the influencing factors, characterized by high accuracy and minimal deviation from the observed data.

5. APPLICATION

To evaluate the accuracy of the proposed fitting formula compared with actual corrosion observed in bridge main cable steel wires, the main cable of the Humen Bridge in China was inspected in late 2017. The analysis involved three steps: (1) determining the corrosion environment at the bridge site, (2) calculating the corrosion-induced mass loss of steel wires over the service period using the fitting formula (Eq. 3), and (3) comparing the results with the actual inspection data from the Humen Bridge.

5.1. Annual spectrum statistics of corrosion environment

As environmental monitoring sensors cannot be directly installed inside the main cable, the temperature and humidity conditions of the outermost steel wires were assumed to represent the overall main cable environment. Environmental factors, including temperature and relative humidity, were extracted from the bridge site's 2017 meteorological records for analysis and simplification. Since corrosion is negligible below the critical relative humidity of 60 %, the analysis focused on a range of 60 % to 100 %, while only temperatures above 0 ℃ were considered based on the experimental setup. Fig. 6 illustrates the distribution and duration of these temperature and relative humidity conditions.

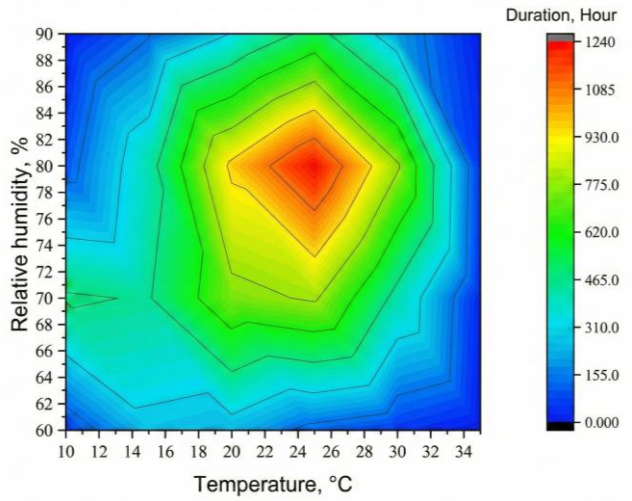

Fig. 6. Annual climate spectrum of temperature and humidity in 2017 at the bridge site

Notes: The maximum temperature of the whole day is set as the continuous temperature of 12 hours during the day, and the minimum temperature is set as the continuous temperature of 12 hours at night.

From Fig. 6, it is evident that approximately 73 % of the year at the bridge site experienced high-temperature (20 – 35 ℃) and high-humidity (70 – 90 %) conditions, a climate conducive to corrosion.

pH value and NaCl concentration: samples of corroded steel wires from the outer layer of the main cable were soaked in 200 mL of ultrapure water for 1 hour. The immersion solution was analyzed, yielding a pH value of 7.26 and an NaCl concentration of 4.1 mg/kg.

Tensile stress: the horizontal component of the main cable force was 265,636.249 kN. Based on the nominal diameter of the steel wires (5.2 mm), the horizontal component of dead load tension of single steel wire was calculated as 898.65 MPa.

5.2. Corrosion calculation

Using the corrosion environment parameters derived above, Eq. 3 was applied to calculate the corrosion rate. Under the combined effects of NaCl concentration (4.1 mg/kg), pH value (7.26), and tensile stress (898.65 MPa), the corrosion rate of the steel wire was determined to be 0.0217 mm/y.

To isolate the contribution of NaCl concentration, pH value, and tensile stress, the influence of temperature and humidity was subtracted using the experimental method described in reference [8]. The relationship between temperature, relative humidity, and corrosion rate was modeled as Eq. 4.

$$\begin{cases} V = 0.0621x_{tem} + 0.0677x_{rh} - 9.7\times10^{-4}x_{tem}^2 \\ \quad -5.5\times10^{-4}x_{rh}^2 - 9\times10^{-5}x_{tem}x_{rh} - 2.409, x_{tem} \in [10^0C, 50^0C], x_{rh} \in [40\%, 60\%] \\ V = 25.549 - 0.298x_{tem} - 0.549x_{rh} + 1.41\times10^{-3}x_{tem}^2 \\ \quad +3.51\times10^{-3}x_{rh}^2 + 3.17\times10^{-3}x_{tem}x_{rh}, x_{tem} \in [10^0C, 50^0C], x_{rh} \in [61\%, 90\%] \end{cases}, \quad (4)$$

where V is the corrosion rate of uncoated smooth high-strength steel wire, mm/y; x_{tem} is the ambient temperature, ℃; x_{rh} is the relative humidity, %.

For experimental conditions of 25 ℃ and 100 % relative humidity, Eq. 4 yielded a corrosion rate of 0.0197 mm/y. By subtracting this value from the total rate (0.0217 mm/y), the corrosion rate due solely to NaCl concentration, pH value, and tensile stress was calculated as 0.002 mm/y.

To estimate the annual corrosion rate under actual service conditions, the statistical annual spectrum of temperature, relative humidity, and their respective durations (as shown in Fig. 6) were substituted into Eq. 4. The resulting corrosion rate distribution is illustrated in Fig. 7.

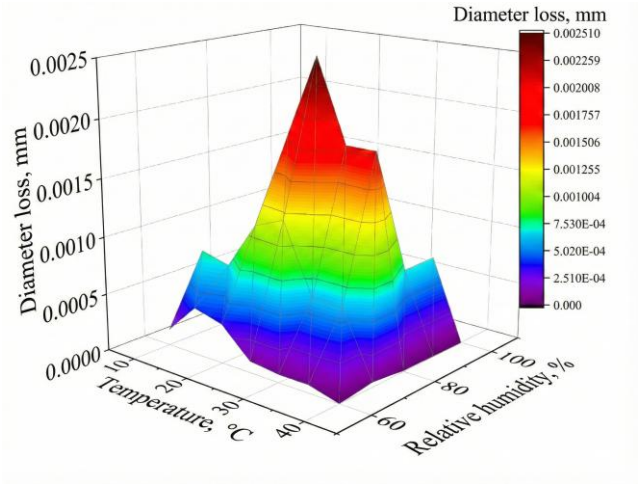

Fig. 7. Annual diameter loss of steel wire in 2017 due to temperature and relative humidity

The calculated average annual diameter loss under the annual environmental spectrum was 0.015 mm, with an additional 0.002 mm attributed to the combined effects of NaCl concentration, pH value, and tensile stress. The total annual diameter loss of the steel wire was approximately 0.017 mm.

5.3. Steel wire corrosion detection of humen bridge

The Humen Bridge was opened to traffic in 1997, utilizing high-strength steel wires with a diameter of 5.2 mm and a standard tensile strength of 1600 MPa for the main cables. After 20 years of operation, an inspection of the midspan section of the bridge's main cable was conducted in December 2017. Fig. 8 and Fig. 9 show photographs from the on-site inspection. As depicted in Fig. 8, the corrosion of the outermost steel wires was severe, and the degree of corrosion increased radially from the interior to the exterior layers of the main cable. The corrosion was classified into four grades, as illustrated in Fig. 9. Fig. 10 provides the distribution of corroded steel wires within the cable.

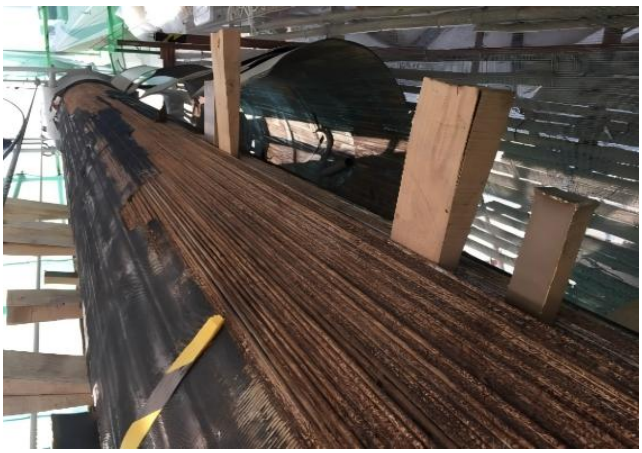

Fig. 8. Corrosion of the outermost steel wires of the main cable

Fig. 9. Classification of corrosion severity in main cable steel wires

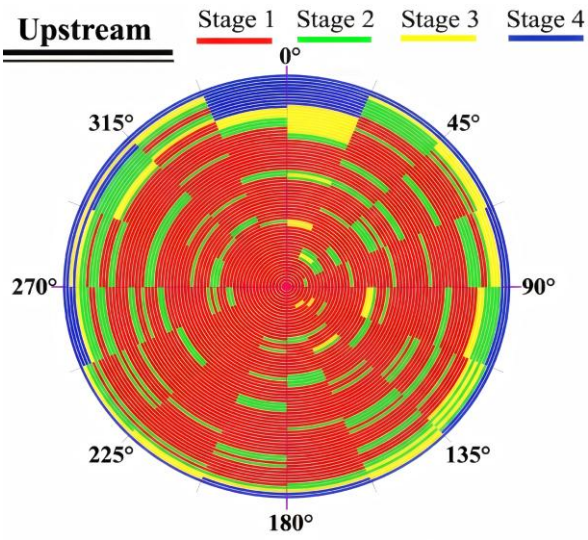

Fig. 10. Distribution of corroded steel wires in the main cable

To further investigate, the corrosion layer thickness of the most severely corroded outermost steel wires was measured. Two 1-cm samples were cut from the steel wires, embedded in epoxy resin mixed with o-benzene and ethylenediamine, and sealed. The cross-sectional micromorphology was observed using a 3D confocal microscope, as shown in Fig. 11. In Fig. 11 a, the cross-sectional micromorphology of sample No. 4-11 reveals that

the rust layer has completely covered the steel wire substrate after the loss of the galvanized layer.

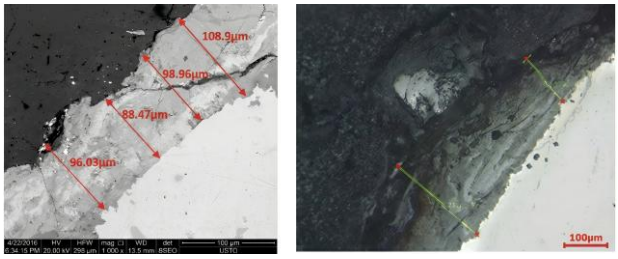

a b

Fig. 11. 3D confocal micrographs of rust layers on steel wire cross-sections: a – the cross-sectional micromorphology of sample No. 4-11; b – the corrosion pit area of the sample No. 4-11

The average thickness of the rust layer was approximately 100 μm. In Fig. 11 b, the corrosion pit area of the same sample shows a maximum corrosion depth of 230 μm. Measurements of three other grade-4 corroded steel wire samples yielded rust layer thicknesses ranging from 100 μm to 200 μm, with steel wire diameter losses of approximately 0.01 mm to 0.2 mm.

5.4. Comparison of calculations with actual bridge corrosion

Since the experimental steel wires used were non-galvanized, the time required for the galvanized layer of the bridge's steel wires to corrode must be deducted before making comparisons. According to 534 report [5] and international inspection practices, the galvanized layer typically corrodes after 6 – 10 years of service. For this analysis, it was assumed that base steel corrosion begins after 10 years of service and that the corrosion environment remains constant over the bridge's 100-year design life.

After 20 years of operation, the base steel wires of the Humen Bridge have been corroding for 10 years. The calculated diameter loss under these conditions is approximately 0.17 mm. Inspection results from the Humen Bridge indicate a corrosion depth of 0.1 mm to 0.2 mm, which aligns well with the calculated values, confirming the reliability of the predictive model.

6. DISCUSSION

This study, through orthogonal experiments and variance analysis, clearly demonstrates the significant influence of pH and NaCl concentration on the corrosion rate of high-strength steel wires. These findings are consistent with previous research, which has established that these two factors are crucial contributors to steel corrosion in marine and coastal environments [11 – 13, 17]. The accelerated dissolution of iron under acidic conditions [11, 17] and the penetration of the passive film on steel by chloride ions, leading to localized corrosion and pitting [12, 13], are well-established principles in corrosion science. It is noteworthy that the influence of tensile stress observed in this study was relatively minor. While some studies suggest that tensile stress can exacerbate corrosion [18], our results indicate that, at least within the tested stress range (400 – 800 MPa), its effect is less pronounced than that of pH and NaCl concentration. This could be attributed to the fact that the applied stress levels, although substantial, remained below the yield strength of the steel. It is conceivable that at higher stress levels, approaching the material's yield point, the influence of tensile stress on corrosion would become more significant, warranting further investigation.

A key finding of this research is the presence of a significant coupling effect between NaCl concentration and pH. The orthogonal experimental design and variance analysis revealed this interaction, which is also reflected in the quadratic terms (x_{NaCl} and x_{pH}) of the fitted model (Eq. 3). This highlights the non-additive nature of these factors, emphasizing the necessity of considering combined environmental effects when assessing corrosion risk. Simply analyzing individual factors in isolation may underestimate the true corrosion rate. Previous related research has not sufficiently quantified this coupling effect [8, 17], and the results of this study underscore its importance.

Compared to prior studies, this research offers the advantage of establishing a quantitative relationship between corrosion rate and the key influencing factors (NaCl concentration, pH, and tensile stress). Previous research often focused on qualitative descriptions of corrosion factors or developed models based on a limited range of environmental conditions, lacking the quantitative precision needed for practical applications [17 – 19]. The fitted calculation model (Eq. 3) developed in this study addresses this gap, providing a quantitative basis for corrosion rate prediction in real-world engineering scenarios. The segmented approach to fitting the model (using different equations for NaCl < 1 % and NaCl ≥ 1 %) reflects the non-linear relationship between NaCl concentration and corrosion rate. This is likely attributable to changes in the corrosion mechanism at different chloride concentrations, as suggested by Kim et al. [13], who observed varied corrosion behaviors at different chloride levels. The corrosion rates observed in our study (0.0087 mm/y to 0.2072 mm/y) are consistent with the range reported in other studies for steel wires under comparable conditions [3, 6, 14]. The validation with data from the Humen Bridge provides further confidence in the model's applicability.

Overall, this study makes significant advancements by quantitatively demonstrating and incorporating the coupling effect of NaCl concentration and pH into a corrosion rate prediction model. The utilization of a self-balanced tension frame for electrochemical corrosion rate measurements under controlled tensile stress represents a novel approach. This method allows for a more accurate simulation of in-service conditions compared to traditional methods where stress is released prior to measurement. This research provides a validated predictive model (Eq. 3) for estimating the corrosion rate of high-strength steel wires in suspension bridge main cables, taking into account the combined effects of NaCl concentration, pH, tensile stress, temperature, and humidity. This model can be used to estimate the remaining service life of main cables and inform maintenance decisions. These findings are of practical importance for bridge maintenance, contributing to a more accurate assessment of bridge cable lifespan.

7. CONCLUSIONS

This study investigated the effects of NaCl concentration, pH value, and tensile stress on the corrosion rate of steel wires using orthogonal experiments. A comparison between the experimental results and the detected corrosion of the Humen Bridge main cables yielded the following conclusions:

1. Influence of Factors: pH value has the most significant influence on steel wire corrosion rate, followed by NaCl concentration. Tensile stress, within the tested range, has a less significant influence. This order of importance contributes to establishing more effective anti-corrosion measures.
2. Coupling Effects: NaCl concentration and pH value exhibit a significant coupling effect on steel wire corrosion, which is more influential than the impact of tensile stress within the range tested. This coupling effect cannot be ignored and is crucial for accurate corrosion prediction.
3. Quantitative Relationships: A quantitative model (Eq. 3) relating the three factors (NaCl concentration, pH value, tensile stress) to the steel wire corrosion rate was established through curve fitting. This model, combined with the temperature and humidity relationship from reference [8], provides a comprehensive predictive method for the corrosion of main cable steel wires in suspension bridges. This method is novel and useful for bridge maintenance.
4. Validation with Humen Bridge Data: Under the environmental conditions of the Humen Bridge, the estimated diameter loss of main cable steel wires is approximately 0.17 mm after 20 years of service. This value aligns well with the observed diameter loss of 0.05 mm to 0.2 mm in the bridge inspection, confirming the reliability of the predictive model. Therefore, the calculated values are considered reliable for predicting steel wire corrosion and advancing the body of scientific knowledge in this area. This allows for a more accurate assessment of bridge cable lifespan.
5. Advancement of Scientific Knowledge: This research has moved the body of scientific knowledge forward by providing a validated, quantitative model that incorporates the crucial coupling effect of pH and NaCl concentration, which has often been overlooked in previous research. The novel experimental setup also improves the accuracy of corrosion rate measurements under realistic service conditions.

REFERENCES

1. **Li, H., Yan, H., Wang, X., Li, L.** Corrosion Fatigue Evaluation of Suspender Cables in Railway Bridges Considering the Effect of Train-Induced Flexural Vibration *Journal of Bridge Engineering* 29 (12) 2024: pp. 04024089. https://doi.org/10.1061/JBENF2.BEENG-6952
2. **Li, R., Wang, H., Miao, C., Ni, Y., Zhang, Z.** Experimental and Numerical Study on the Degradation Law of Mechanical Properties of Stress-Corrosion Steel Wire for Bridge Cables *Journal of Constructional Steel Research* 212 2024: pp. 108294. https://doi.org/10.1016/j.jcsr.2023.108294
3. **Zhao, Y., Su, B., Fan, X., Yuan, Y., Zhu, Y.** Corrosion Fatigue Degradation Characteristics of Galvanized and Galfan High-Strength Steel Wire *Materials* 16 (2) 2023: pp. 708. https://doi.org/10.3390/ma16020708
4. **Deng, L., Deng, Y.** Study on Multi-Crack Damage Evolution and Fatigue Life of Corroded Steel Wires inside in-Service Bridge Suspenders *Applied Sciences* 14 (20) 2024: pp. 9596. https://doi.org/10.3390/app14209596
5. **Jiang, C., Wu, C., Cai, C., Jiang, X., Xiong, W.** Corrosion Fatigue Analysis of Stay Cables under Combined Loads of Random Traffic and Wind *Engineering Structures* 206 2020: pp. 110153. https://doi.org/10.1016/j.engstruct.2019.110153
6. **Li, R., Wang, H., Miao, C., Yuan, Z., Zhang, Z.** Three-Dimensional Fatigue Crack Initiation and Propagation Behavior of Stress-Corroded Steel Wires for Bridge Cables *International Journal of Fatigue* 192 2025: pp. 108717. https://doi.org/10.1016/j.ijfatigue.2024.108717
7. **Shen, M., Deodatis, G., Betti, R., Blabac, B., Martin, B.** A Novel Methodology for Inspection and Strength Evaluation of Suspension Bridge Main Cables *Journal of Structural Engineering* 149 (8) 2023: pp. 04023107. https://doi.org/10.1061/JSENDH.STENG-11891
8. **Xin, F., Han, Y., Zhang, G.** Inspection and Corrosion Rule of Parallel Steel Wire Main Cables of Suspension Bridge in Service *Journal of Water Resources and Architectural Engineering* 15 (3) 2017: pp. 118 – 122.
9. **Miyachi, K., Chryssanthopoulos, M., Nakamura, S.** Experimental Assessment of the Fatigue Strength of Corroded Bridge Wires Using Non-Contact Mapping Techniques *Corrosion Science* 178 2021: pp. 109047. https://doi.org/10.1016/j.corsci.2020.109047
10. **Wang, D., Wang, B., Xie, G., Li, C., Zhang, D., Ge, S.** Effect of Temperature on Tribo-Corrosion Behaviors of Parallel Steel Wires of Main Cable in the Suspension Bridge *Wear* 512 2023: pp. 204522. https://doi.org/10.1016/j.wear.2022.204522
11. **Eghbali, F., Moayed, M.H., Davoodi, A., Ebrahimi, N.** Critical Pitting Temperature (Cpt) Assessment of 2205 Duplex Stainless Steel in 0.1 M Nacl at Various Molybdate Concentrations *Corrosion Science* 53 (1) 2011: pp. 513 – 522. https://doi.org/10.1016/j.corsci.2010.08.008
12. **Ebrahimi, N., Momeni, M., Moayed, M.H., Davoodi, A.** Correlation between Critical Pitting Temperature and Degree of Sensitisation on Alloy 2205 Duplex Stainless Steel *Corrosion Science* 53 (2) 2011: pp. 637 – 644. https://doi.org/10.1016/j.corsci.2010.10.009
13. **Kim, H., Nam, J., Kwon, S.** Corrosion Behavior of Astm A416 Tendon Steel in Wet Conditions under Various Chloride Concentrations *International Journal of Electrochemical Science* 19 (10) 2024: pp. 100808. https://doi.org/10.1016/j.ijoes.2024.100808
14. **Xue, S., Shen, R., Chen, W., Miao, R.** Corrosion Fatigue Failure Analysis and Service Life Prediction of High Strength Steel Wire *Engineering Failure Analysis* 110 2020: pp. 104440. https://doi.org/10.1016/j.engfailanal.2020.104440
15. **Guo, T., Liu, Z., Correia, J., de Jesus, A.M.** Experimental Study on Fretting-Fatigue of Bridge Cable Wires *International Journal of Fatigue* 131 2020: pp. 105321. https://doi.org/10.1016/j.ijfatigue.2019.105321

16. **Xue, S., Shen, R.** Corrosion-Fatigue Analysis of High-Strength Steel Wire by Experiment and the Numerical Simulation *Metals* 10 (6) 2020: pp. 734. https://doi.org/10.3390/met10060734
17. **Li, R., Miao, C., Wei, T.** Effect of Environmental Factors on Electrochemical Corrosion of Galvanized Steel Wires for Bridge Cables *Anti-Corrosion Methods and Materials* 69 (1) 2022: pp. 111 – 118. https://doi.org/10.1108/ACMM-07-2021-2522
18. **Li, R., Miao, C., Wei, T.** Experimental Study on Corrosion Behaviour of Galvanized Steel Wires under Stress *Corrosion Engineering, Science and Technology* 55 (8) 2020: pp. 622 – 633. https://doi.org/10.1080/1478422X.2020.1769273
19. **Jie, Z., Zhang, Z., Susmel, L., Zhang, L., Lu, W.** Corrosion Fatigue Mechanisms and Evaluation Methods of High-Strength Steel Wires: A State-of-the-Art Review *Fatigue & Fracture of Engineering Materials & Structures* 47 (7) 2024: pp. 2287 – 2318. https://doi.org/10.1111/ffe.14311